Characterization of Room Impulse Response System on the Application of Varied Width Unit Step Signals in a Noisy Environment

BHUVNESH KUMAR SHARMA, MITHILESH KUMAR, R.S. MEENA
Department of Electronics Engineering,
Rajasthan Technical University Kota,
Kota, Rajasthan,
INDIA.

Abstract: In this paper, the response of the room impulse response system for the various-width pulse signal input is represented in a discrete-time domain. The result shows that the response is a low pass filter. The phase response of the system comes out as a minimum phase for the input of different pulse widths. The phase response is piecewise linear. A FIR model is given to implement the room impulse response. Analysis of the room impulse response system for AWGN, Rayleigh, Exponential, and Poisson noise are also given here. It is observed from the results that as the signal-to-noise ratio increases, the maximum amplitude of output also increases but the shape of the curve remains constant. At the same time, the phase response is piecewise linear.

Keywords: Finite Impulse Response, Image source method, Piecewise linear, Room acoustic, Room Impulse Response (RIR).

Received: April 27, 2024. Revised: November 19, 2024. Accepted: December 11, 2024. Published: December 31, 2024.

1. Introduction

Characterization of a digital system gives an understanding of the processing capabilities of that system for the basic input signals. It provides an understanding about the system's Magnitude and Phase response in both time and frequency domain. The unit step response of a system shows its behavior on the application of the sudden change at the input. Unit step analysis provides an insight into the system's capabilities, and limitations and helps to optimize and troubleshoot the system with known parameters.

The idea of RIR is used to represent a mathematical model for the acoustic properties of a room or a closed space. It is a time-varying response between a sound source and a microphone. Acoustic characteristics of a room are defined as the RIR and it depends upon the room size, surface, material, shape, position of sound energy source, and the listener's position in a closed room. The above information is required in various acoustic applications such as acoustic noise cancellation, and acoustic feedback cancellation, to improve the audio and speech quality in a communication system and for sound system optimization. The virtual and Augmented reality environment also be created with the help of the RIR function. RIR measurement is typically done by specialized equipment or software. To calculate the acoustic properties of a room, the understanding of RIR provides a tool for easy simulation of the acoustic nature of that room, in the field of research and engineering.

The unwanted effect in an acoustic system such as feedback, Echo, or reverberation can be easily removed or controlled by calculating the RIR for that particular environment. Various measurement techniques and mathematical models are traditionally used to calculate RIR. In many applications, the acoustic characteristics of the environment are required. Many techniques are used to calculate these characteristics from the acoustic measurements. To calculate the RIR a fast neural diffuse RIR generator is provided in [1] for a given acoustic scenario. In this paper, a neural network method is given for generating RIR for rectangular rooms. The result shows that the fast diffuse RIR generator is faster than a diffuse acoustic simulator. A Process to reconstruct direct and reverberant sound fields with early reflections of sound field and near field sources with some prior knowledge for automatic speech recognition experiments discussed in [2], which shows that the computational complexity is reduced when the system has some knowledge about the source position, geometry of the room and the errors are also reduced. An inverse method to calculate absorption coefficients which are frequency dependent for walls of a room, ceiling, and the floor of the room with the help of several RIR measurements given in [3]. A method for generating actual synthetic RIR by using an adversarial network RIR generator (IR-GAN) is given in [4], which reports that the IR-GAN provides an error rate lower than an acoustic simulator based on the geometry of a cuboid room. A data set of measured room impulse response is provided in [5]. It includes attenuations at the microphone and source positions and the image source in different wall positions. A method to calculate the direction of sound rays and the early reflection delay for a single source to remove the limitations of existing solutions is provided in [6] as phase phase-aligned correlation method. A fast implementation technique is given in [7] to calculate the RIR by multiple images of the source with a graphic data Processing Unit to reduce the computation speed of the image source method. A technique to find room geometry from acoustic

impulse response is provided in [8]. To make the real RIR and the calculated RIR near to each other a technique and architecture is discussed in [9]. It uses a synthetic RIR and translates it into an actual RIR. A review to calculate the room acoustics for small rooms is provided in [10].

To recognize the image sources by knowing the of room impulse responses is given in [11]. To identify and estimate the room impulse response a Kronecker product decomposition method is provided in [12] for multi-dimension system. When a sound source moves freely in a closed room then the estimation of RIR is required to be calculated at different positions and continuously updated. A method to estimate the RIR for new sound source locations is provided in [13]. Room acoustic Parameters changes as the room dimensions and the environmental conditions changes. The reverberation time depends upon the room's temperature and room's humidity of the room. A study to show the effect of humidity and temperature on reverberation time was provided in [14]. The estimation method for the RIR with the help of sparse Bayesian learning is given in [15]. To augment the special characteristics of the RIR by using simulated RIR is given in [16]. Different algorithm comparison for acoustic simulation for better accuracy is provided in [17]. The frequency domain simulation method to remove the unwanted effects from the RIR is given in [18]. A comparison between different methods to find the decay of room modes is given in [19]. Here ray tracing image source method is used to estimate the mathematical model of RIR.

In the first part of this paper, a simple discussion of the RIR is given. Then a discrete time function for RIR is given and the output of the RIR system for the different width pulse signal is shown. In the second part of the paper, the RIR output for a fixed-width pulse signal in the presence of AWGN noise is demonstrated.

From the literature survey, it is found that traditionally RIR is used in various acoustic applications such as acoustic Echo cancellation, feedback cancellation, and noise cancellation. Here the use of RIR as a digital system is considered. The development of a system to separate the speech signal is provided in [20]. This model uses a blind source separation technique in the frequency domain to separate the sound source. The transfer function of RIR depends upon the room dimensions, environmental conditions, and the distance between the receiver and the source. When RIR is used as a digital system these parameter works as the control parameter for that system and by changing these parameter values the characteristics of RIR are also changed. The basic behaviour of the RIR is as a notch filter which has the minimum phase response. When the control parameters are changed the position of notch shifts. Phase response of RIR comes as piecewise linear. It is a well-known fact that the knowledge of Impulse response and unit step response of a digital system helps to find out the system behaviour for unknown input. Here unit step response of RIR in the presence of different noises is shown.

2. The Image Method for Room Impulse Response

A mathematical function between the microphone and loudspeaker in a room represents the RIR in a closed box-shaped room. When in a room loudspeaker and a microphone are placed in different locations the sound energy generated by the loudspeaker is collected by the microphone, but before this sound energy is received by the microphone, it takes multiple paths. Some sound energy is directly received by the microphone from the source and some energy is received by the microphone after going through multiple times reflections from the walls of the room. The amplitude of these reflected rays depends upon the number of reflections it takes before reaching the microphone, the reflection coefficient of the walls, room temperature, and the velocity of the sound in those particular environmental conditions. The Image source method is generally employed to estimate the relation between the emitted sound energy by the loudspeaker and the collected sound energy by the microphone. This function represents the room impulse response. By increasing the number of reflections, the total distance traveled by sound ray before being collected by the microphone increases and so the amplitude of that particular sound ray decreases. A diagram for second-order virtual sources to estimate the RIR function by image method is as below:

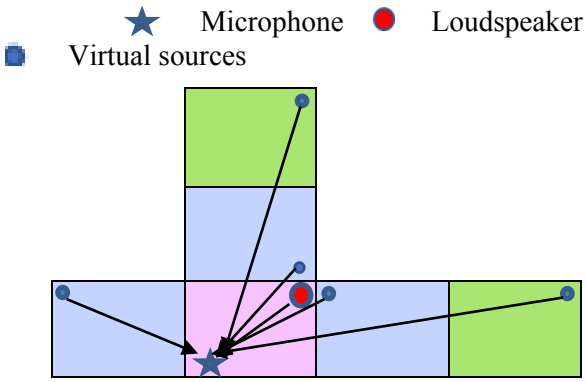

Fig. 1 Second-order virtual source representation to estimate the RIR.

Mathematically the room impulse response function in discrete time can be written as:

$$h[n] = \sum_{a=-q}^{q} \sum_{b=-q}^{q} \sum_{c=-q}^{q} z_{abc}\, e\left[\frac{n}{f_s} - \frac{p_{abc}}{s_{air}}\right] \quad (1)$$

- n represents sampling instance.
- f_s represents sampling frequency.
- p_{abc} shows the distance covered by echo ray.
- s_{air} shows sound velocity.
- a is the index for the x direction of ^{the} virtual source.
- b is the index for the y direction of b^{th} virtual source.
- c is the index for the z-direction of c^{th} virtual source.
- q represents total number of reflections and estimated as q=|a|+|b|+|c|.
- z_{abc} shows the magnitude of the echo.

Echo amplitude changes on changing the reflection coefficients of the walls and the dimensions of the room. Here magnitude and phase plot for room impulse response for a = 1, b=c=0 is as in Figure 2&3 and corresponding parameters are as in Table 1. When the number of reflections are increased, the complexity of the model increases by many folds. So, for demonstration purpose room impulse response is demonstrated only for two-dimensional reflections.

Table 1: Different parameters for the calculation of RIR System

Sampling frequency for RIR measurement in Hz	410
Room Dimensions for RIR measurement in meters	5,5,6
The microphone's dimensions in meters	3,3,4
The loudspeaker's dimensions in meters	4,4,4
The reflection coefficient of the room walls	0.3
Order of virtual sources	1
Room temperature in ^{0}C	27

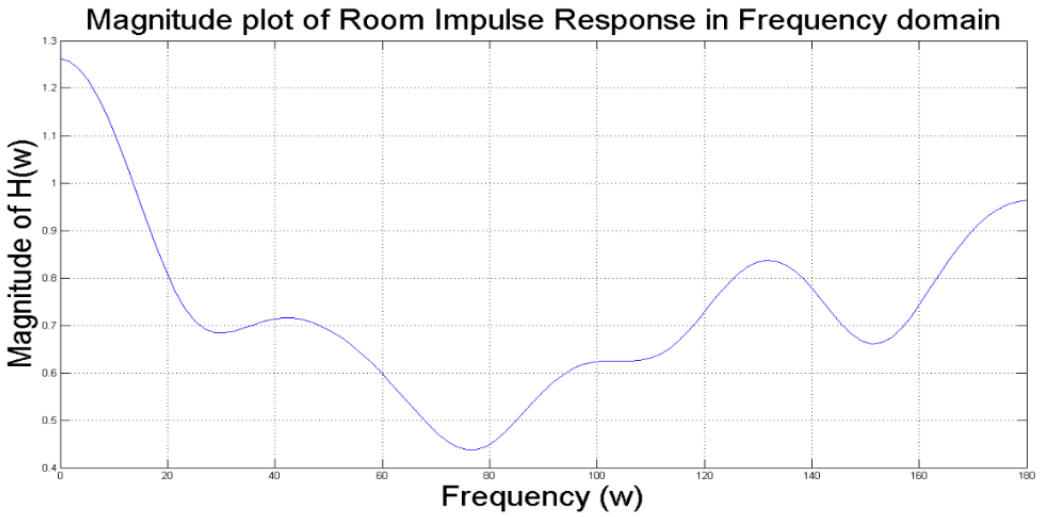

Fig. 2 Magnitude plot of room impulse response

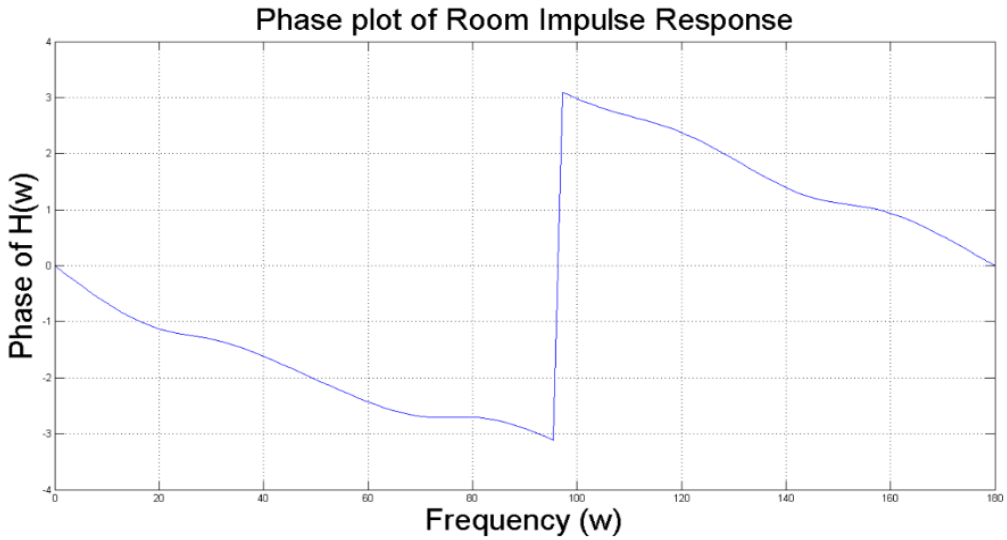

Fig. 3 Phase plot of room impulse response

3. The System Model

In this section, a direct form FIR filter structure is proposed to implement the room impulse response for equation (1). The direct structure is used to represent the filter because the direct structures are very easy to implement and have low complexity. If RIR system h(n) has M distinct values, then this structure requires M number of memory elements, M additions, and M multiplications per output point. The proposed Finite impulse response (FIR) structure for room impulse response is shown in Figure 4 (a), (b) the output of the RIR system for unit step signal sequence U(n) can be written as:

$$y\ [n] = \sum_{k=0}^{M-1} h[k]\, u\,[n-k] \qquad (2)$$

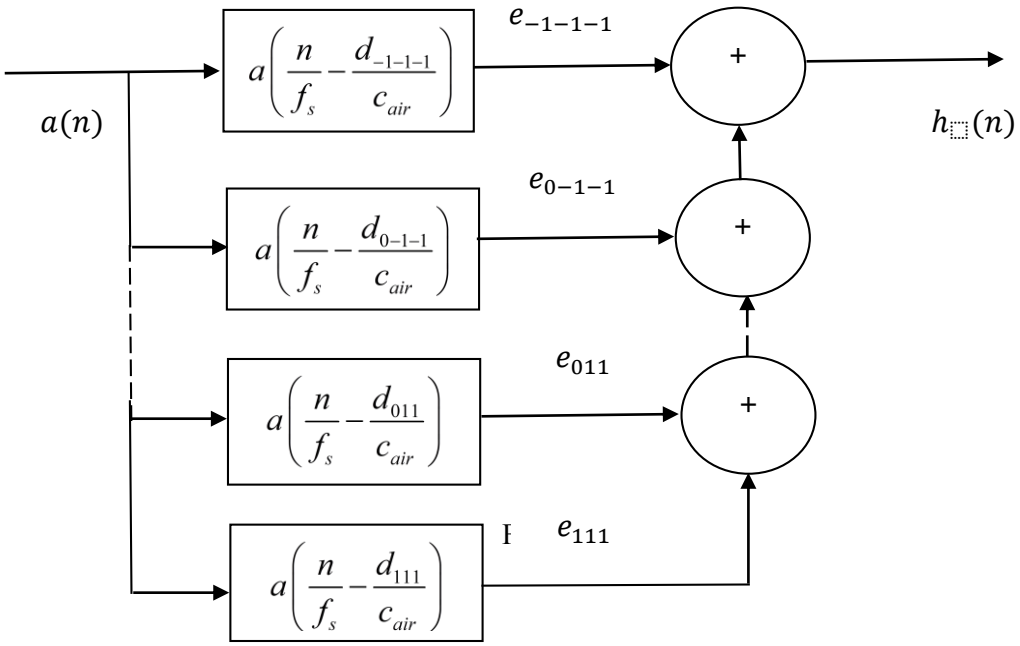

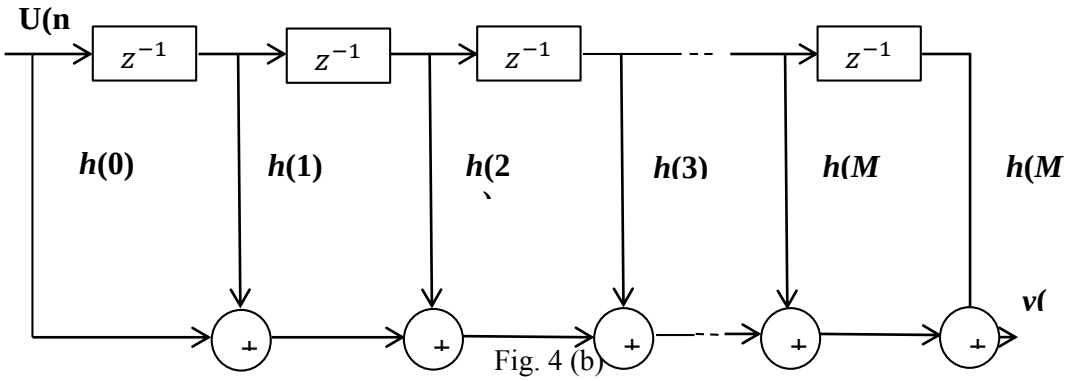

Fig. 4 (b)

Fig. 4 (a), (b) The proposed FIR structure for RIR

Where h(k), for k=0,1,…M-1 represents the sum of all ray's magnitudes reaches to the microphone at time index k.

4. System With Minimum Phase

A system with minimum phase is generally a useful characteristic of linear time-invariant system. If any system satisfies the causality and the stability then the system shows minimum phase response. When the system response is minimum phase then the phase prediction of the output signal is very easy, which is used for the various applications of the system design.

$$u(t)=\begin{cases}0, & \text{if } t<0\\ 1, & \text{if } t\geq 0\end{cases} \quad (3)$$

For discrete time domain unit step signal is generally used to calculate the output of a system for an abrupt change in the input and it also characterizes the system and is used to explain the system transient response.

5. Phase and Magnitude Response H(N) for Unit Step Signal

To calculate the response of a RIR for different unit step signals, the input is defined as follows:

$$u_1[n]=\sum_{k=0}^{4}u[k]\,\delta\,[n-k] \quad (4)$$

$$u_2[n]=\sum_{k=0}^{12}u[k]\,\delta\,[n-k] \quad (5)$$

$$u_3[n] = \sum_{k=0}^{20} u[k]\,\delta\,[n-k] \quad (6)$$

$$u_4[n] = \sum_{k=0}^{28} u[k]\,\delta\,[n-k] \quad (7)$$

The total length of the input sequence is 32 taken for calculation. The RIR systems response $u_{ai}[n]$ of $h[n]$ for a given unit step input are shown as:

$$h[n] = x_r[n] + jx_i[n] \quad (8)$$

$$u_{ai}[n] = (x_r[n] + jx_i[n]) * u_i[n] \quad (9)$$

$$u_{ai}[n] = (x_r[n]) * u_i[n] + (jx_i[n]) * u_i[n] \quad (10)$$

$$|u_{a1}(n)| = \sqrt{\left(\sum_{k=0}^{4} u_1[k]x_r(n-k)\right)^2 + \left(\sum_{k=0}^{4} u_1[k]x_i[n-k]\right)^2}\ ,\ Ru_{a1}(n) = \tan^{-1}\left(\frac{\sum_{k=0}^{4} u_1[k][n-k]}{\sum_{k=0}^{4} u_1[k]x_r[n-k]}\right) \quad (11)$$

$$|u_{a2}[n]| = \sqrt{\left(\sum_{k=0}^{12} u_2[k]x_r[n-k]\right)^2 + \left(\sum_{k=0}^{12} u_2[k]x_i[n-k]\right)^2}\ ,\ Ru_{a2}[n] = \tan^{-1}\left(\frac{\sum_{k=0}^{12} u_2[k]x_i[n-k]}{\sum_{k=0}^{12} u_2[k]x_r[n-k]}\right) \quad (12)$$

$$|u_{a3}[n]| = \sqrt{\left(\sum_{k=0}^{20} u_3[k]x_r[n-k]\right)^2 + \left(\sum_{k=0}^{20} u_3[k]x_i[n-k]\right)^2}\ ,\ Ru_{a3}[n] = \tan^{-1}\left(\frac{\sum_{k=0}^{20} u_3[k]x_i[n-k]}{\sum_{k=0}^{20} u_3[k]x_r[n-k]}\right) \quad (13)$$

$$|u_{a4}[n]| = \sqrt{\left(\sum_{k=0}^{28} u_4[k]x_r[n-k]\right)^2 + \left(\sum_{k=0}^{28} u_4[k]x_i[n-k]\right)^2}\ ,\ Ru_{a4}[n] = \tan^{-1}\left(\frac{\sum_{k=0}^{28} u_4[k]x_i[n-k]}{\sum_{k=0}^{28} u_4[k]x_r[n-k]}\right) \quad (14)$$

Table 2 Estimated values of $u_{ai}(n)$ for different width unit step inputs

Input unit step Width	Max. Magnitude	Cutoff Frequency in (radians)
5	6.30	14.4
13	16.40	10.8
21	26.50	7.2
29	36.59	5.4

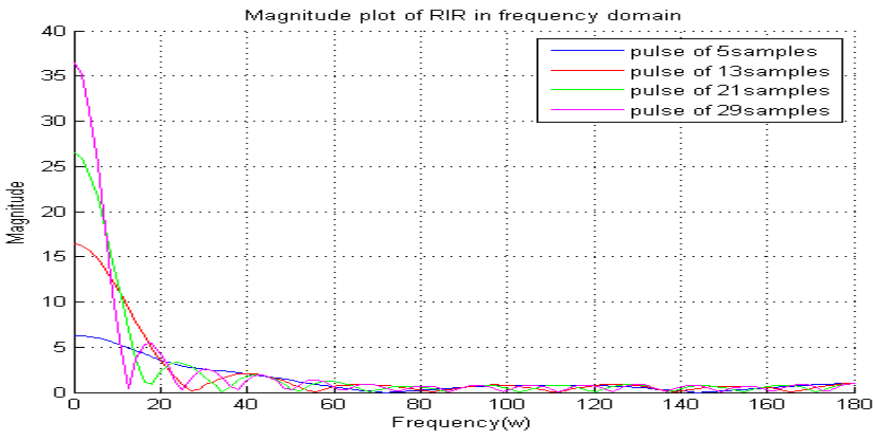

Fig. 5 Magnitude plot of the output for different unit step signals of RIR

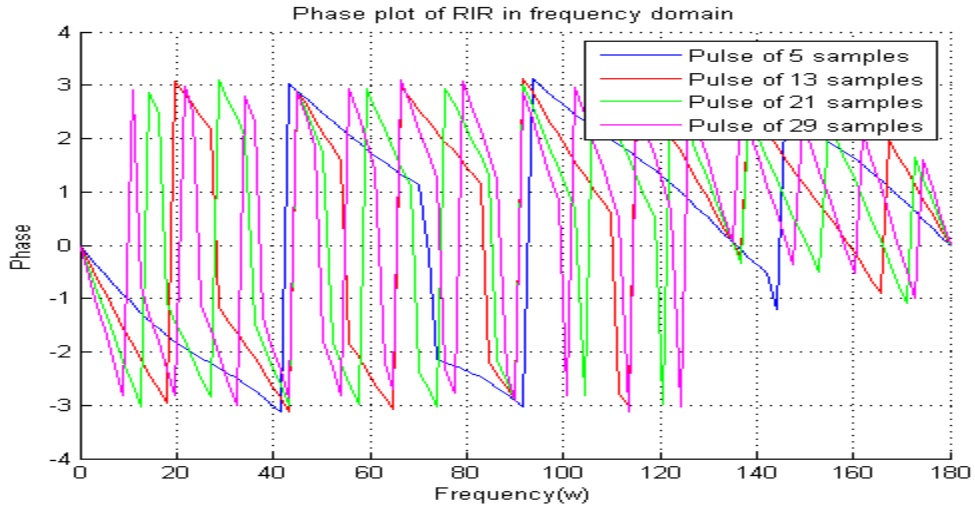

Fig. 6 Phase plot of the output for different unit step signals of RIR

The behavior of RIR for the different unit step signals is shown in Figure 5&6. The input signal to the RIR has the pulse width of 5, 13, 21, and 29 samples. It is clearly observed from Figure 5 that behavior of the room impulse response system is a low pass filter for the various width input Pulse signals and from Figure 6 phase response is the minimum phase. The phase response is also piecewise linear for a particular duration output of room impulse response.

6. RIR Behaviour Analysis in Noisy Environment

Here characterization of the RIR system is given for different noises. In a communication system, there are four common types of noises that are generally studied to find out the response of the system and to make adjustments in our transmitted signal and the behavior of the system to mitigate the effects produced by the noise. The common noises are AWGN noise, Rayleigh noise, Poisson noise, and exponential noise.

7. AWGN Noise

In a communication system, Additive White Gaussian (AWGN) noise generally represents the effect of random disturbances in the system. It is an additive noise, which means it is added to the each and every sample of the signal and it has the Gaussian distribution. It has a flat frequency spectrum means the power is equally distributed in all frequency components of the noise. The variance of the Gaussian distribution represents the noise power. Often AWGN noise is used to model mathematically the real-world noise in communication systems. AWGN is generally used for simulating a communication system for random noise.

Here noise is Gaussian distributed with zero mean. The power spectral density function for Gaussian distribution is:

$$f_g(y) = \frac{1}{\sqrt{2\pi\sigma_g}} \exp\left[-\frac{\left(y-\mu_g\right)^2}{2\sigma_g^{\,2}} \right]$$

(15)

μ_g=mean

$\sigma_g^{\,2}$=variance

Here we take mean = 0

$$\text{signal to noise ratio} = 10\log 10 \frac{A^2}{\sigma_g^{\,2}}$$

(16)

It is clearly observed from the figure 6 that the energy in the main lob of the output decreases on decreasing signal-to-noise ratio (SNR) from +5 db to -4db.

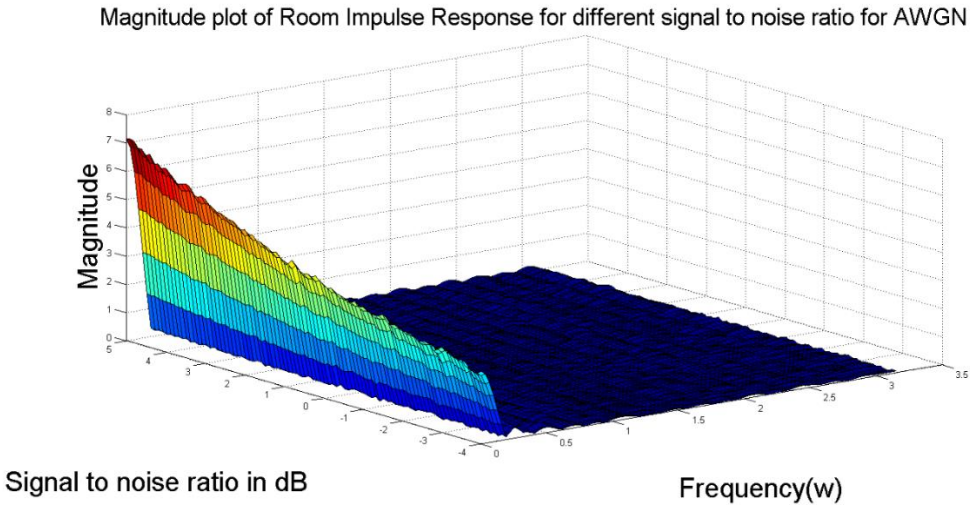

Fig. 7 Magnitude plot of RIR for different signal-to-noise ratio for AWGN

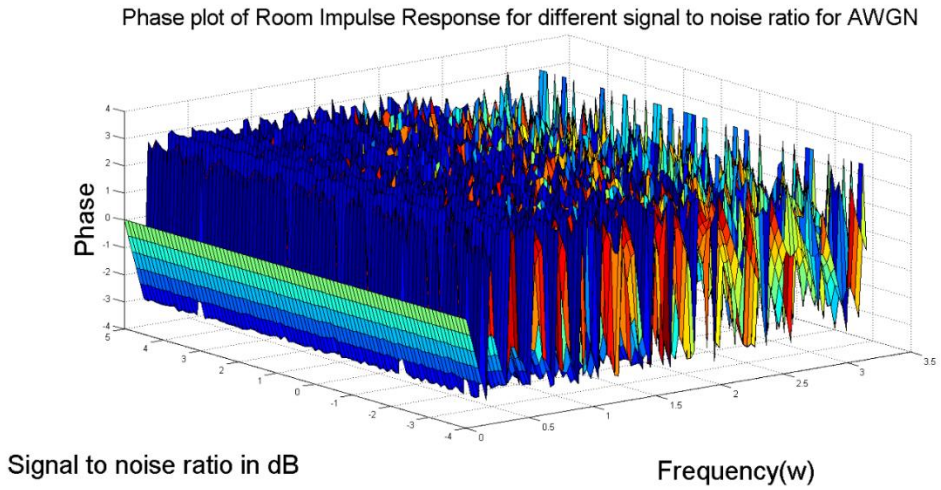

Fig. 8 Phase plot of RIR for different signal-to-noise ratios for AWGN

8. Rayleigh noise in communication systems

Rayleigh noise is a random variation in the amplitude of a wave, which is produced when the signal wave propagates through a wireless medium. It is basically the scattering of the radio waves by the small objects in the propagation medium between the transmitter and receiver. when a wave scatters in the propagation medium then it is received at the receiver by following different paths and different phase waves are received at the point of receiver, which causes the fading. The special case of two waves with diffuse power fading is called Rayleigh fading. This Reyleigh fading has a significant effect in wireless communication systems and many times it drops the signal completely. It is also producing errors in data transmission. The probability density function for Rayleigh distribution is:

$$f_r(x) = \frac{x}{b^2} e^{\left(-\frac{x^2}{2b^2}\right)}$$

(17)

b = parameter

$$\text{signal to noise ratio} = 10\log 10 \frac{A^2}{n_r}$$

(18)

A = Amplitude of the signal

nr=Rayleigh noise power

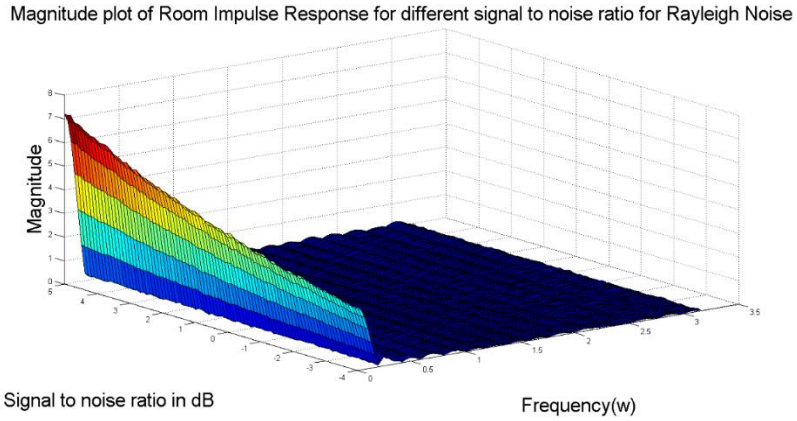

Fig. 9 Magnitude plot of RIR for different signal-to-noise ratio for Rayleigh noise.

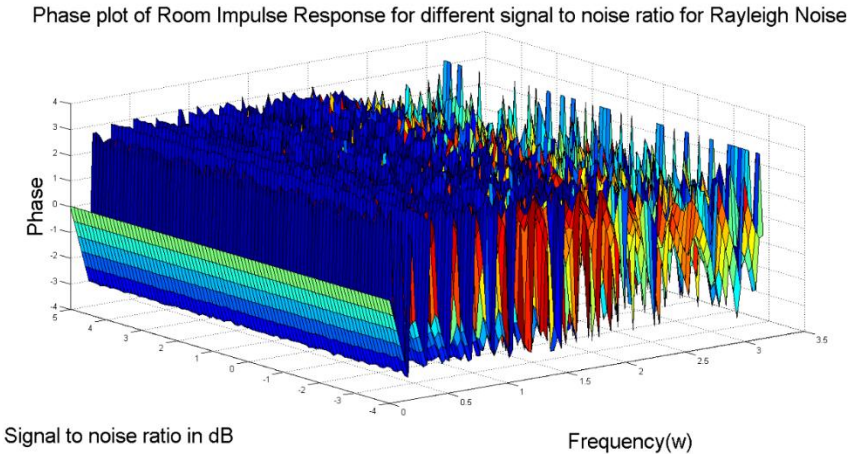

Fig. 10 Phase plot of RIR for different signal-to-noise ratio for Rayleigh noise.

9. Poisson noise

In an optical communication system when the signal is transmitted in the form of light the poison noise occurs due to the transmitted photons Random behavior in travelling in the optical medium and arrive at the receiver in a random manner. Most commonly this poison noise is studied in optical communication system

The Poisson distribution is defined as:

$$f_p(k) = \frac{\mu^k}{\lfloor k} e^{-\mu} \quad (19)$$

μ=parameter

$$\text{signal to noise ratio} = 10\log 10 \frac{A^2}{n_p} \quad (20)$$

A= Amplitude of the signal

np= Poisson noise power

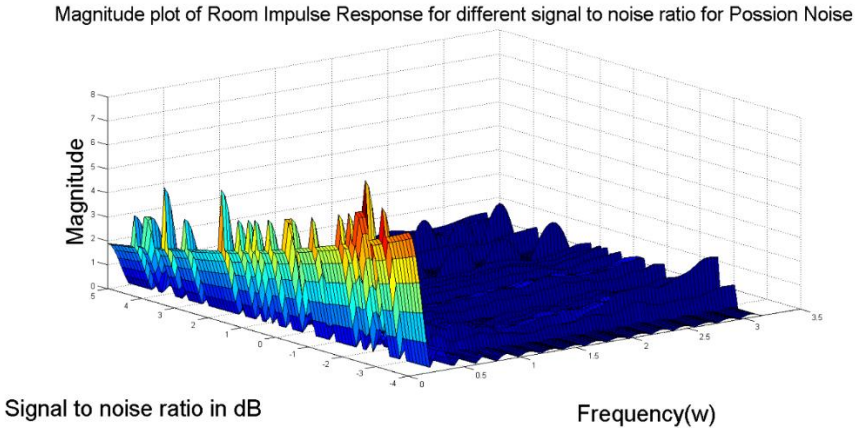

Fig. 11 Magnitude plot of RIR for different signal-to-noise ratios for Poisson noise.

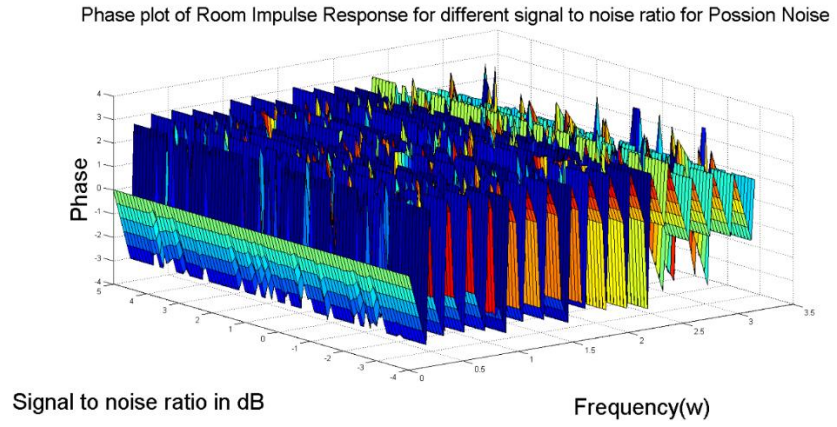

Fig. 12 Phase plot of RIR for different signal-to-noise ratios for Poisson noise.

10. Exponential noise

Exponential noise occurs in a communication system because of random variations in the signal amplitude due to the sources of interference, shot noise, thermal noise and other random processes. The exponential density function is defined as:

$$f_e(k) = \frac{1}{b} e^{-\frac{(k-a)}{b}} \quad (21)$$

Equation (21) defined for k > a and for k < a $f_e(k)=0$

$$\text{signal to noise ratio} = 10\log 10 \frac{A^2}{n_e} \quad (22)$$

A= Amplitude of the signal

n_e= exponential noise power

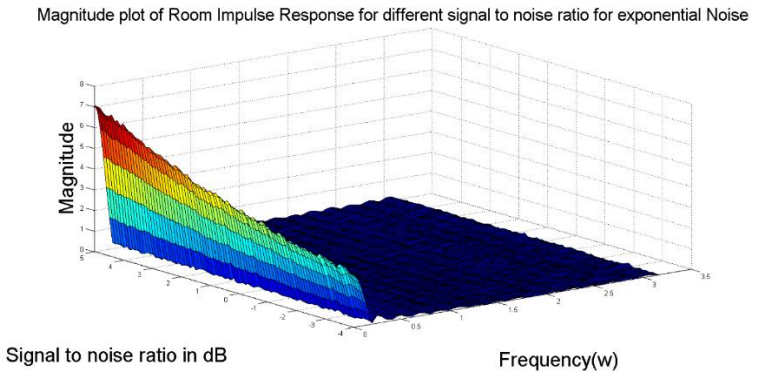

Fig. 13 Magnitude plot of RIR for different signal-to-noise ratio for Exponential noise.

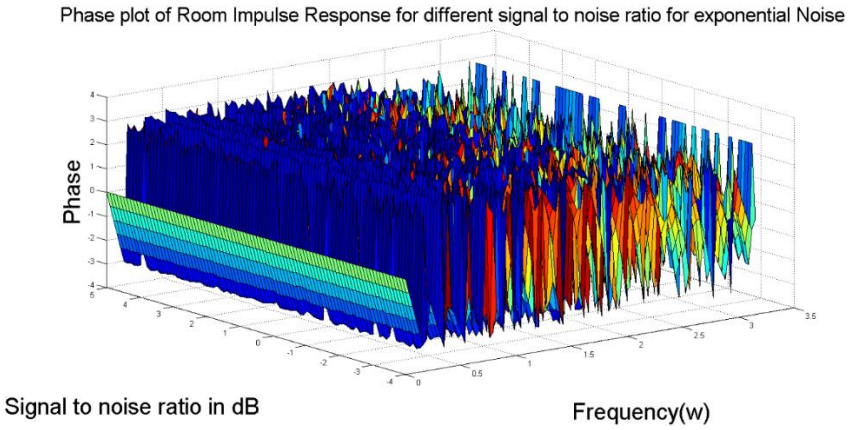

Fig. 14 Phase plot of RIR for different signal-to-noise ratios for Exponential noise.

11. Conclusion

The magnitude plot of room impulse response is successfully demonstrated. From the phase and magnitude plots for different width unit pulse signals, it is observed that the behavior of the room impulse response system for the different width unit pulse signals is as a low pass filter, and phase response is found to be minimum phase. For different widths of the unit pulse signal the phase response of the RIR system behaves as piecewise linear and all the phases start from the 0 and end to the 0 phase. From the magnitude and phase plot in the presence of AWGN noise, the size and the maximum value of RIR output is decreases on decreasing the signal-to-noise ratio + 5 dB to - 4 dB. It also shows that the energy in the main lobe is also decreases with decrease of signal-to-noise ratio. The room impulse response maintains its low pass characteristics for all values of AWGN. This same magnitude and phase response of RIR for the Rayleigh noise shown, for the Poisson noise, for the exponential noise can be easily observed by the corresponding magnitude and phase plots.

References

[1] Anton Ratnarajah, Shi-Xiong Zhang, Meng Yu, Zhenyu Tang, Dinesh Manocha, Dong Yu, "Fast-Rir: Fast Neural Diffuse Room Impulse Response Generator. IEEE International Conference on Acoustics," Speech and Signal Processing (ICASSP), IEEE, pp.571-575, 2022.

[2] Stefano Damiano, Federico Borra, Alberto Bernardini, Fabio Antonacci, Augusto Sarti "Sound field Reconstruction in Reverberant Rooms Based on Compressive Sensing And Image-Source Models Of Early Reflections," IEEE Workshop on Applications of Signal Processing to Audio and Acoustics, New Paltz, NY, USA, 2021.

[3] Stephane Dilungana, Cedric Foy, Sylvain Faisan, "Geometry-Informed Estimation of Surface Absorption Profiles from Room Impulse Responses," 30th European Signal Processing Conference (EUSIPCO), IEEE, 2022.

[4] Anton Ratnarajah, Zhenyu Tang, Dinesh Manocha, "IR-GAN: Room impulse response generator for far-field speech recognition," INTERSPEECH 2021, Brno, Czechia, pp.286-290, 2021.

[5] Diego Di Carlo, Pinchas Tandeitnik, Ce Foy, Nancy Bertin, Antoine Deleforge and Sharon Gannot, "A calibrated room impulse response dataset for echo-aware signal processing," EURASIP Journal on Audio, Speech, and Music Processing, pp.1-15, 2021.

[6] Tom Shlomo, Boaz Rafaely, "Blind Localization of Early Room Reflections Using Phase Aligned Spatial Correlation," IEEE Transactions On Signal Processing, Vol. 69, pp.1213-1225, 2021.

[7] David Diaz-Guerra, Antonio Miguel, Jose R. Beltran1, "A python library for room impulse response simulation with GPU acceleration," Multimedia Tools and Applications, Springer, https://doi.org/10.1007/s11042-020-09905-3, 2020.

[8] Fabio Antonacci, Jason Filos, Mark R. P. Thomas, Emanuel, A. P. Habets, Augusto Sarti, Patrick A. Naylor, Stefano Tubaro, "Inference of Room Geometry From Acoustic Impulse Responses," IEEE Transactions On Audio, Speech, And Language Processing, Vol. 20, No. 10, pp.2683-2695, 2012.

[9] Anton Ratnarajah, Zhenyu Tang, Dinesh Manocha, "TS-RIR: Translated Synthetic Room Impulse Responses For Speech Augmentation," 2021 IEEE Automatic Speech Recognition and Understanding Workshop (ASRU), 10.1109/ASRU51503.2021.9688304, 2022.

[10] Annika Neidhardt, Christian Schneiderwind, Florian Klein, "Perceptual Matching of Room Acoustics for Auditory Augmented Reality in Small Rooms - Literature Review and Theoretical Framework," Trends in Hearing, Vol. 26, pp.1–22, 2022.

[11] Tom Sprunck, Antoine Deleforge, Member, Yannick Privat, Cédric Foy, "Gridless 3D Recovery of Image Sources From Room Impulse Responses," IEEE signal processing letters, vol. 29, pp.2427-2431, 2022.

[12] Laura-Maria Dogariu, Jacob Benesty, Constantin Paleologu, Silviu Ciochina, "Identification of Room Acoustic Impulse Responses via Kronecker Product Decompositions," IEEE/ACM transactions on audio, speech, and language processing, vol. 30, pp.2828-2841, 2022.

[13] Hualin Ren, Christian Ritz, Jiahong Zhao, Daeyoung Jang, "Impact of Compression on the Performance of the Room Impulse Response Interpolation Approach to Spatial Audio Synthesis," APSIPA ASC 2022, pp.442-448, 2022.

[14] Artur Nowo´swiat, "Impact of Temperature and Relative Humidity on Reverberation Time in a Reverberation Room," Buildings (MDPI), 12, 2022.

[15] Maozhong Fu, Jesper Rindom Jensen, Yuhan Li1, Mads Græsboll Christensen, "Sparse modeling of the early part of noisy room impulse responses with sparse bayesian learning," ICASSP 2022 IEEE, pp.586-590, 2022.

[16] Yuichiro Koyama, Kazuhide Shigemi, Masafumi Takahashi, Kazuki Shimada, Naoya Takahashi, Emiru Tsunoo, Shusuke Takahashi, Yuki Mitsufuji, "Spatial data augmentation with simulated room impulse responses for sound event localization and detection," ICASSP 2022 IEEE, pp.8872-8876, 2022.

[17] Eric Brandao, Edna S.O. Santos, Viviane S.G. Melo, Roberto A. Tenenbaum, Paulo H. Mareze, "On the performance investigation of distinct algorithms for room acoustics simulation," Applied Acoustics 187 (2022) 108484, pp.1-12, 2022.

[18] Kohei Yatabe, Akiko Sugahara, "Convex-optimization-based post-processing for computing room impulse response by frequency-domain FEM," Applied Acoustics 199 (2022) 108988, pp.1-16, 2022.

[19] Luka Curovic, Jure Murovec, Tadej Novakovic, Rok Prislan, Jurij Prezelj, "Time–frequency methods for characterization of room impulse responses and decay time measurement," Measurement 196 (2022) 111223, pp.1-17,2022.

[20] Bhuvnesh Kumar Sharma, Mithilesh Kumar, R. S. Meena, "Development of a speech separation system using frequency domain blind source separation technique, Multimedia Tools and Applications," Vol. 83, pp. 32857–32872, 2024.

Contribution of Individual Authors to the Creation of a Scientific Article (Ghostwriting Policy)

The authors equally contributed in the present research, at all stages from the formulation of the problem to the final findings and solution.

Sources of Funding for Research Presented in a Scientific Article or Scientific Article Itself

No funding was received for conducting this study.

Conflict of Interest

The authors have no conflicts of interest to declare that are relevant to the content of this article.